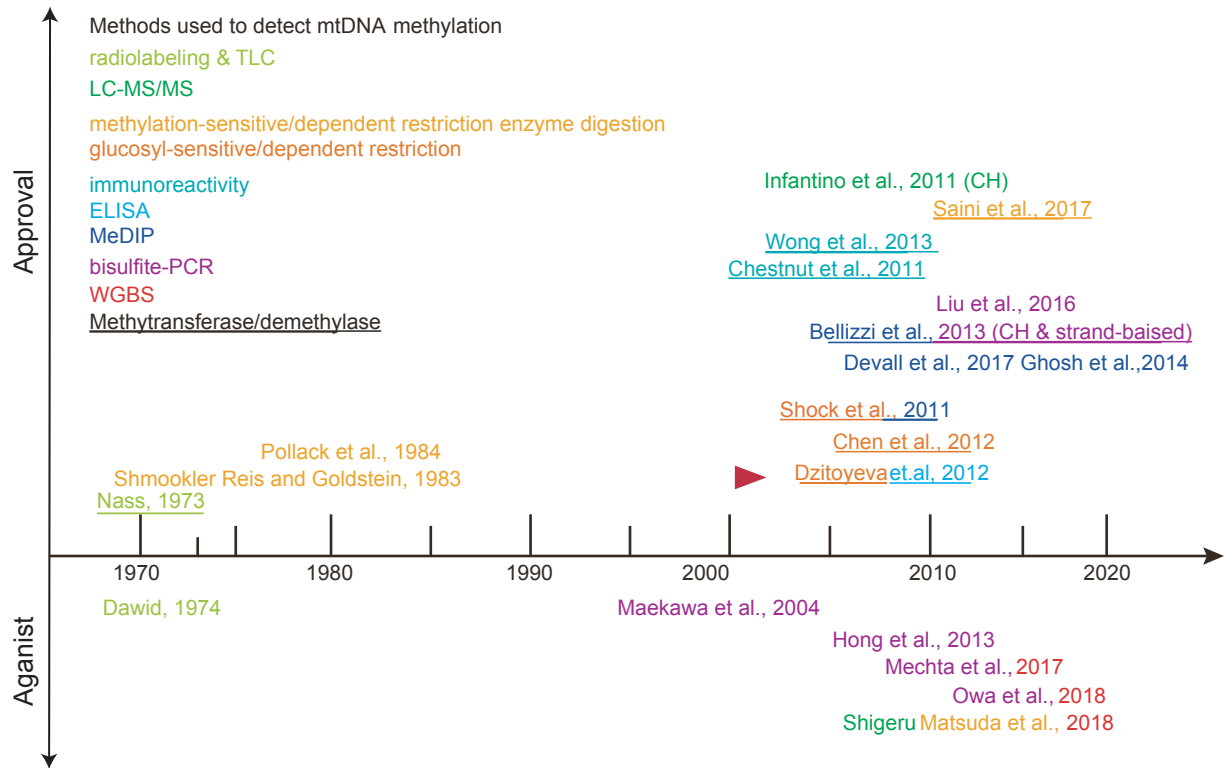


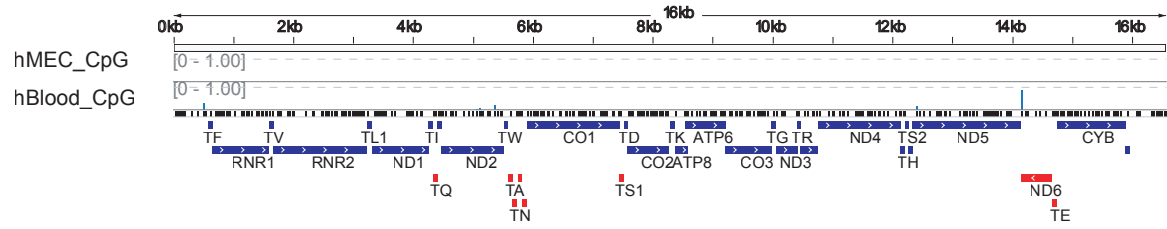
A



B

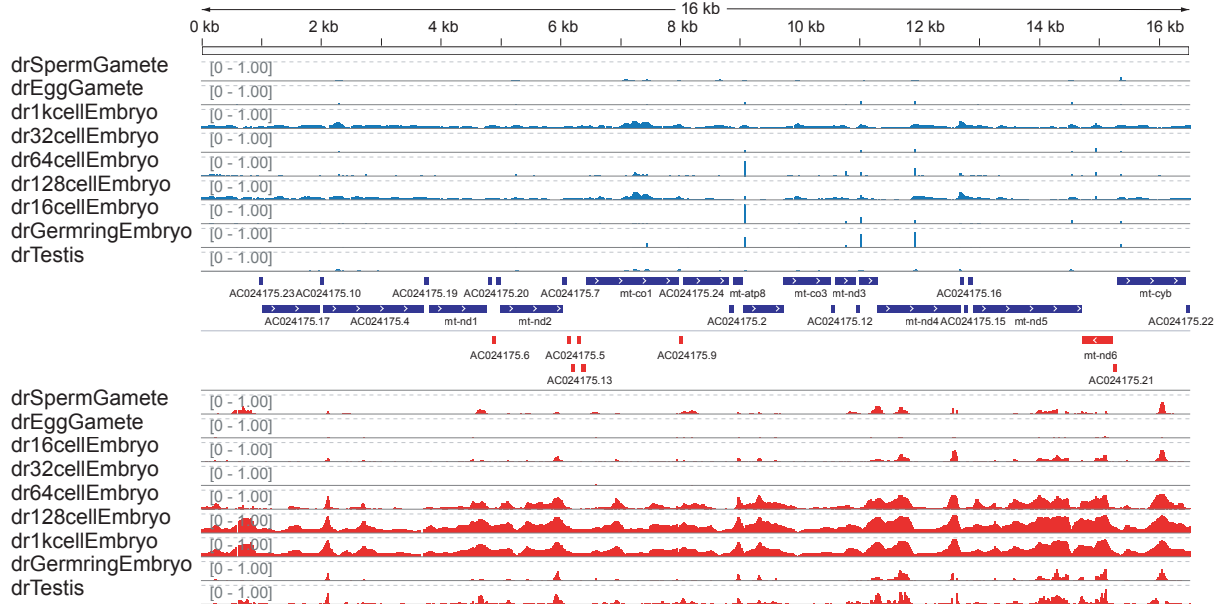
Method	H strand (red) / L strand (blue)	Next generation sequencing	Analytical limitations for mtDNA methylation	mtDNA methylation can be detected
WGBS	1st: NaHSO <sub>3</sub> H: "CAA" C "C" CAGGCATAATTA AACT L: GTT G G GTCCGTATTAATTGA		1. Focus was on CpG methylation instead of all cytosine methylation. 2. Mean mtDNA methylation used instead of single-base analysis. 3. Separate analysis of strand methylation neglected.	YES
RRBS	1st: Digestion (MspI) H: "CAA" C "C" CAGGCATAATTA AACT L: GTT G G GTCCGTATTAATTGA		1. Insufficient MspI restriction sites to cover mtDNA.	NO
BS & PCR-seq	1st: NaHSO <sub>3</sub> 2nd: PCR for certain region H: "CAA" C "C" CAGGCATAATTA AACT L: GTT G G GTCCGTATTAATTGA		1. Primers designed to capture CpGs assuming all CpH are unmethylated thus bias against CpH methylated reads 2. Few loci and small range covered by primers	NO
MeDIP-seq	1st: ChIP (5mC antibody) H: "CAA" C "C" CAGGCATAATTA AACT L: GTT G G GTCCGTATTAATTGA		1. Broad resolution cannot determine single base status. 2. Strands are combined.	YES
MRE-Seq	1st: Digestion (FspEI) H: "CAA" C "C" CAGGCATAATTA AACT L: GTT G G GTCCGTATTAATTGA		1. Cannot detect all methylated C sites	YES

C



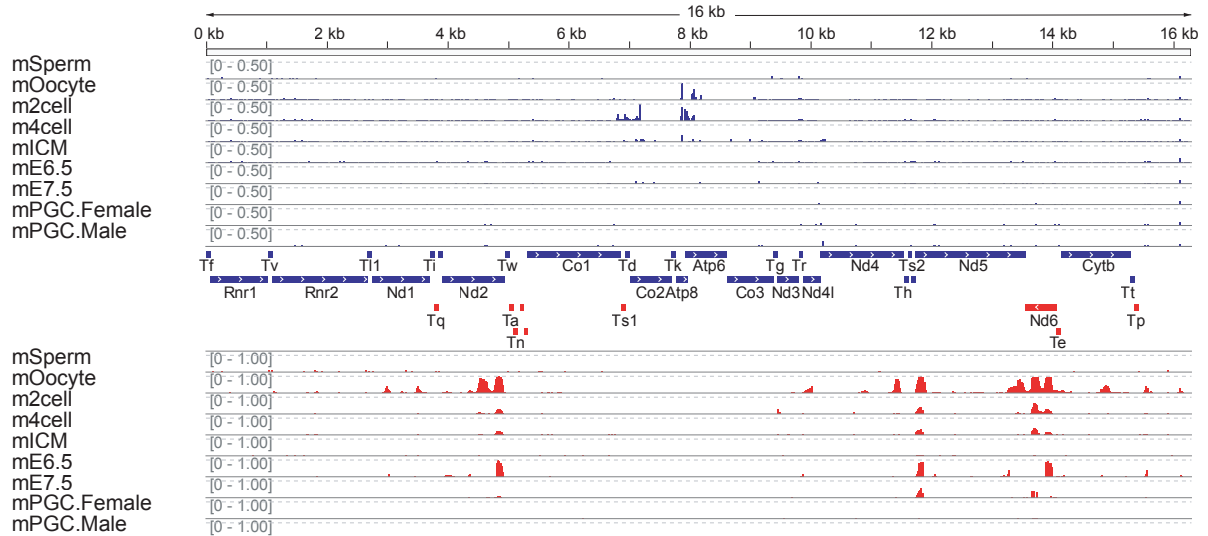
D

NUMTs were removed through mapping to zebrafish whole genome



E

NUMTs were removed through mapping to mouse whole genome



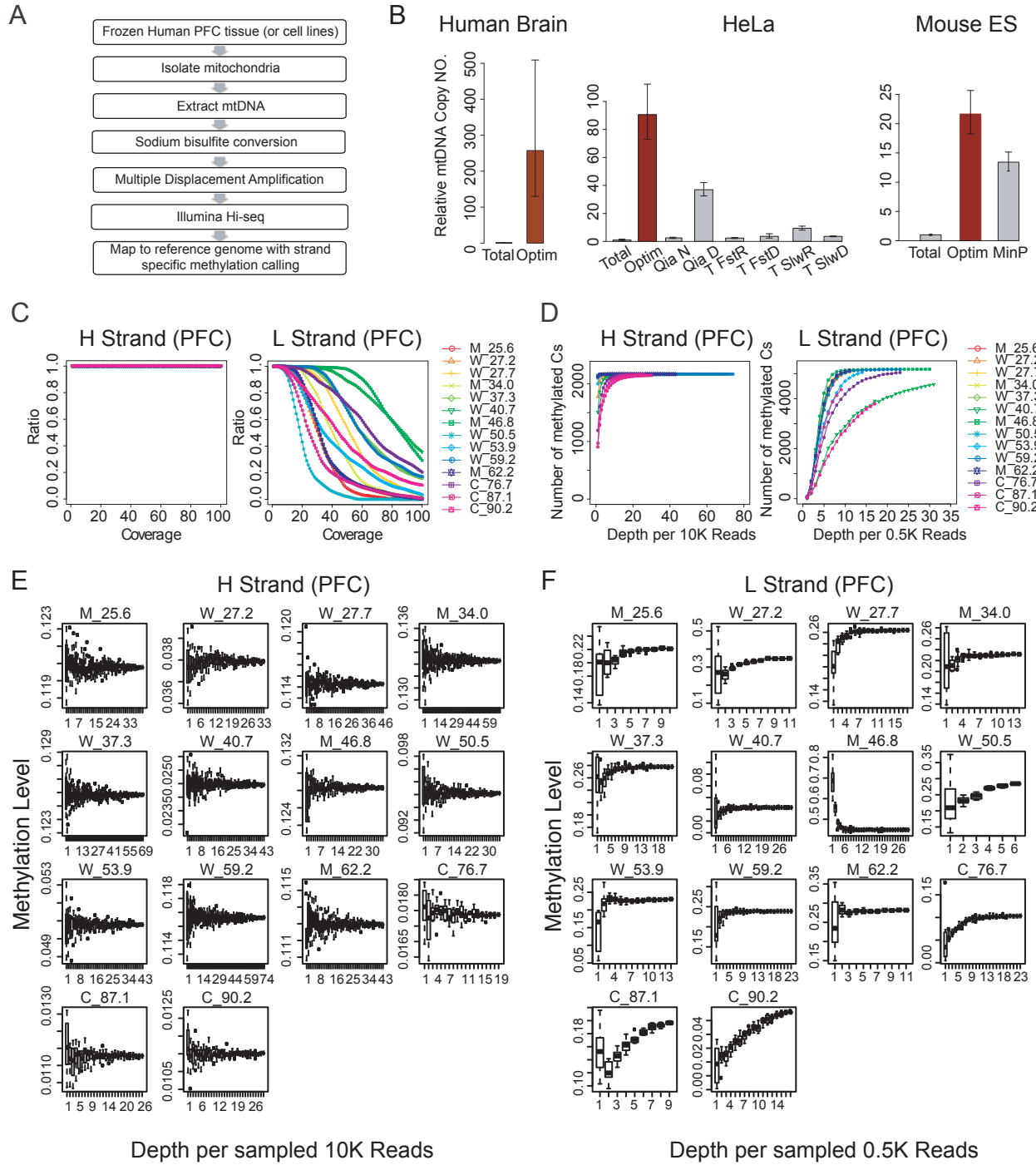
**Supplemental Fig. 1. WGBS of mtDNA quality control.**

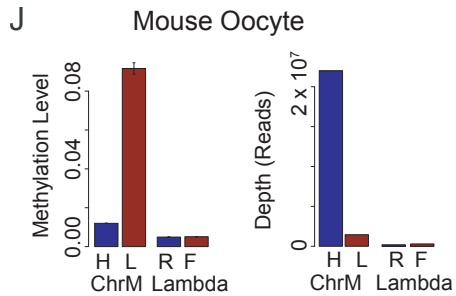
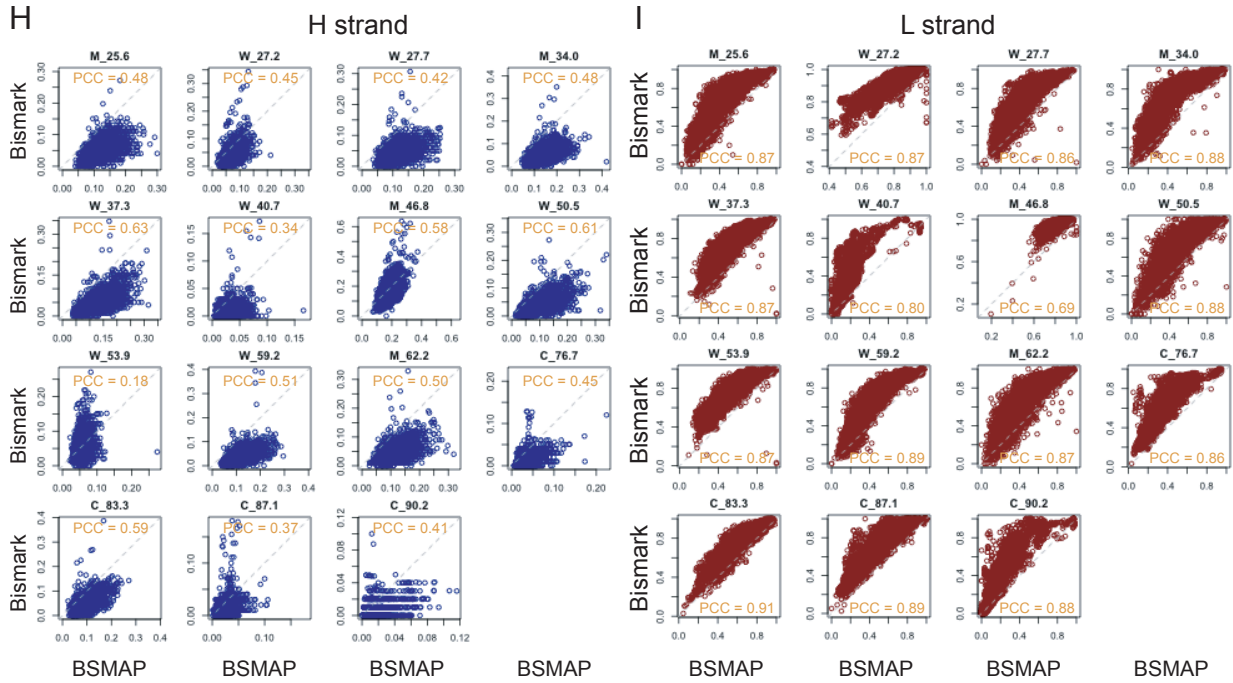
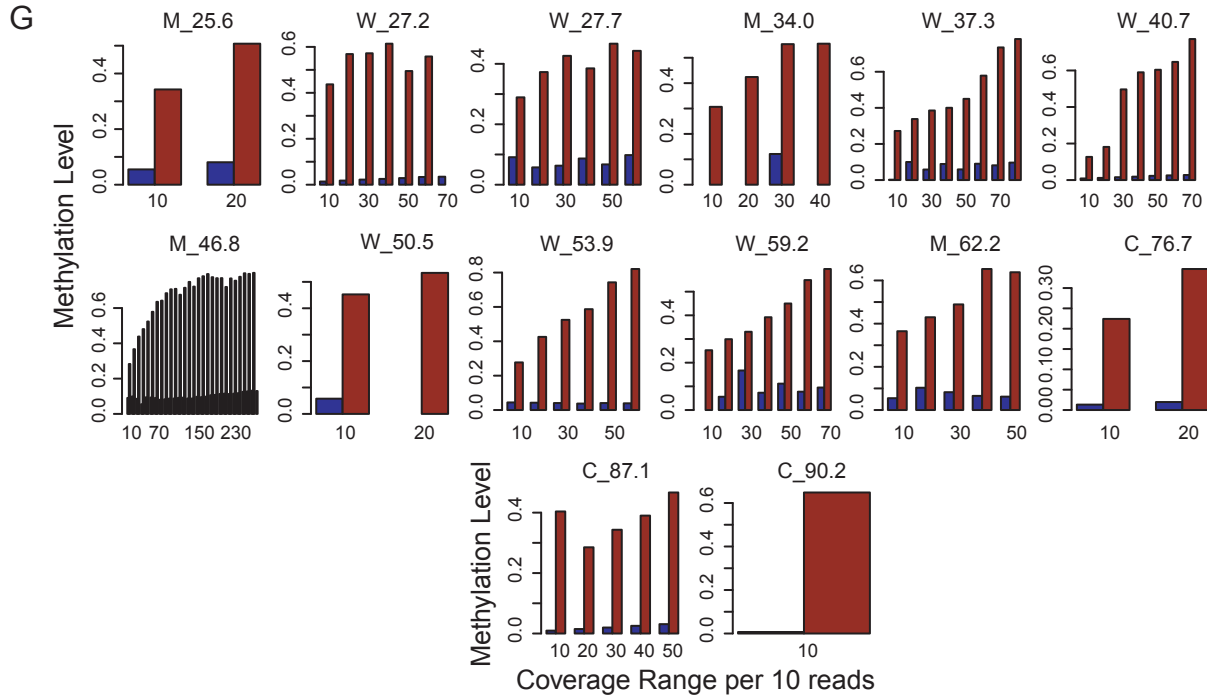
(A) Summary of literature evidence for presence or absence of mtDNA methylation.

(B) Analytical limitation of different methods in detecting mtDNA methylation.

(C) BS-seq methylation (WGBS) profiles of linearized mtDNA in human B cells (GSM922328 under GSE37578) and mammary epithelial cells (MEC, GSM721195 under GSE29127) on only CG sites.

(D-E) BS-seq (WGBS) methylation profiles of linearized mtDNA in zebrafish (D) as in Figure 1B, and mouse (E) as in Figure 1C embryonic development with NUMTs removed through mapping to whole genome.





**Supplemental Fig. 2. WGBS of hPFC mtDNA quality control.**

(A) The mtDNA enrichment and whole mtDNA BS-seq workflow.

(B) Relative mtDNA copy number enrichment using specified mtDNA isolation techniques in HeLa and mouse ES cells.

(C) BS-seq read coverage on mtDNA. Coverage (x-axis) is the number of reads that cover a certain position. Ratio (y-axis) is number of positions with certain coverage divided by length of mtDNA.

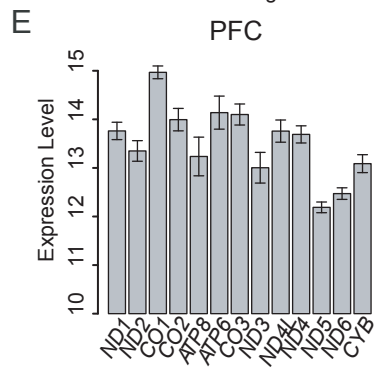
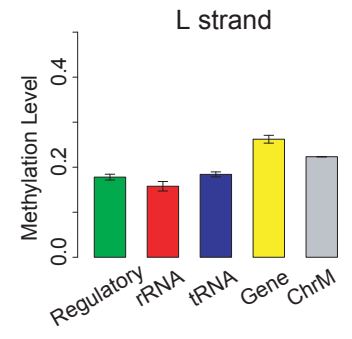
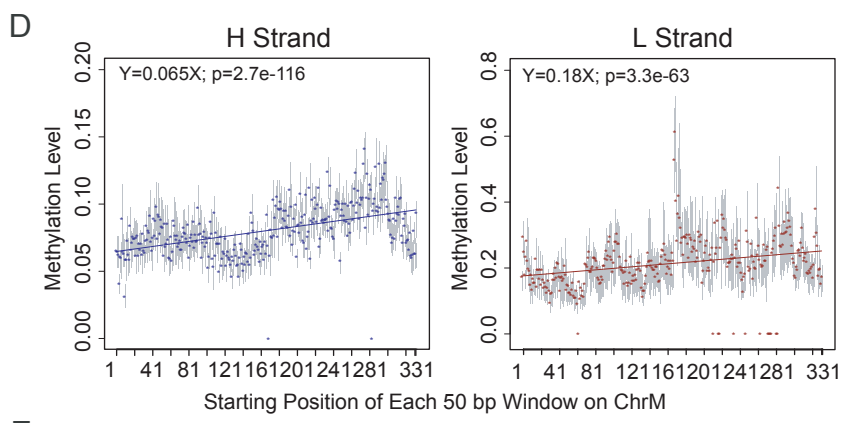
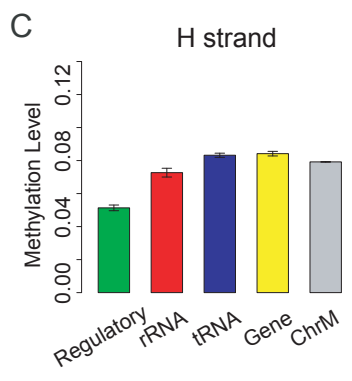
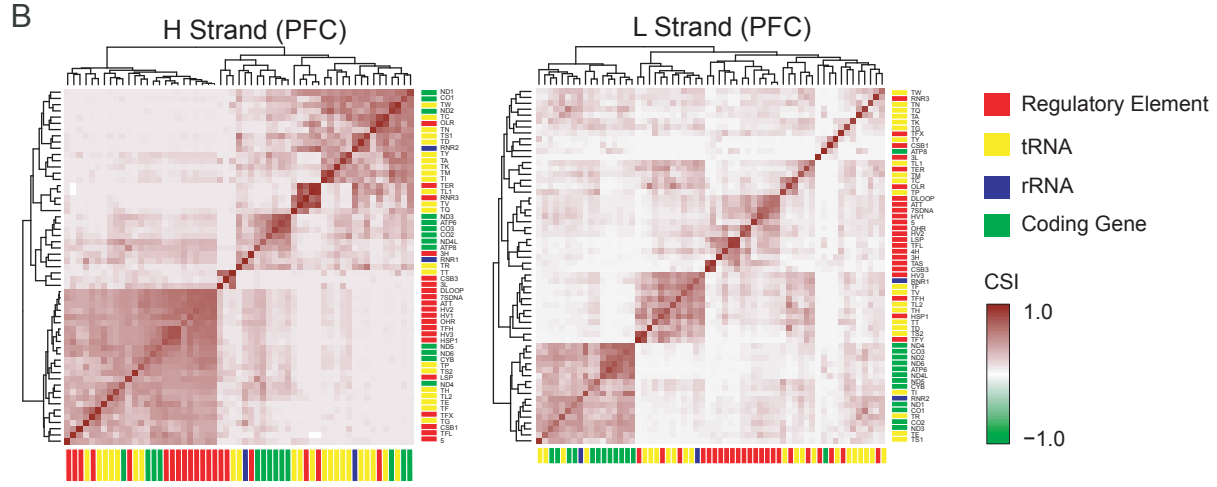
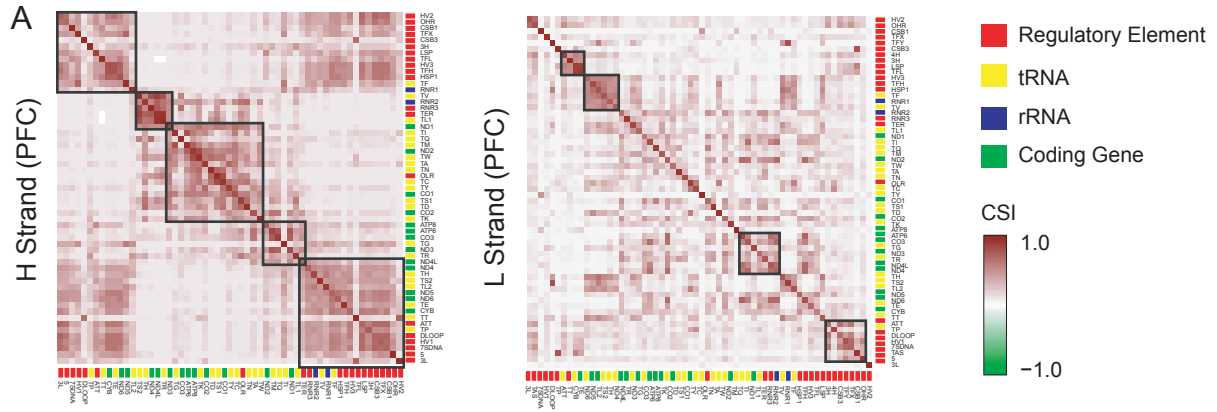
(D) Saturation plots for number of covered Cs by at least 10 reads, from cumulative random sampling of a subset of reads in 10,000 (10k) read blocks for H strand (left panel), or 5000 (0.5k) for L strand (right panel).

(E-F) Saturation plots for mean methylation level of Cs covered by at least 10 reads, from cumulative random sampling of a subset of reads in 10,000 (10k) read blocks for H strand (E), or 5000 (0.5k) for L strand (F).

(G) Methylation level of C on H and L strand with similar coverage.

(H-I) Correlation of mtDNA methylation called by BSMAP and Bismark on H (H) and L strand (I) separately, before any further filtering.

(J) Strand specific methylation level and sequence depth on ChrM, and non-strand specific methylation level and sequence depth on lambda DNA. Error bars represent SEM among C sites covered by at least ten reads.



**Supplemental Fig. 3. Methylation patterns and features across mtDNA in human brain.**

(A) Heat maps of correlation (CSI) between mean methylation level of each functional element across 14 human PFC samples within the H strand or L strand. Functional elements are ordered based on their position on the reference genome (rCRS).

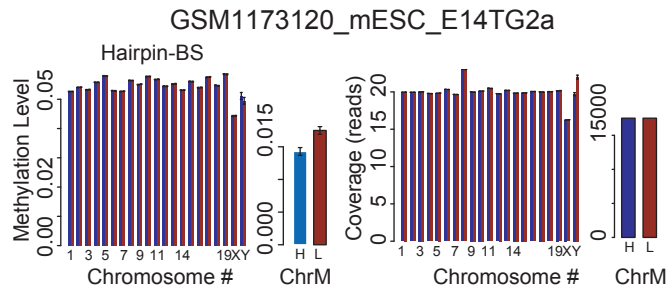
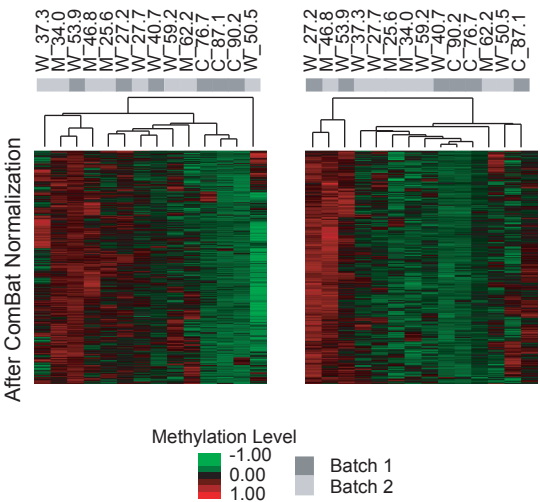
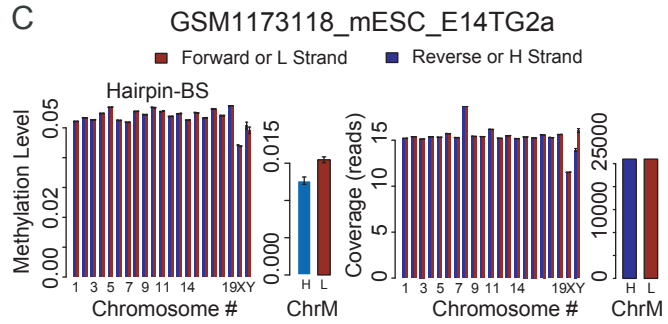
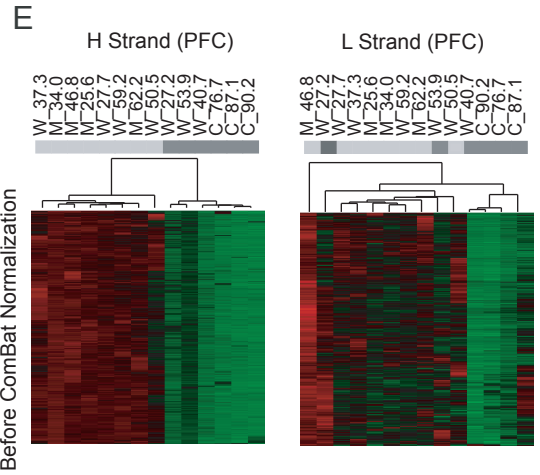
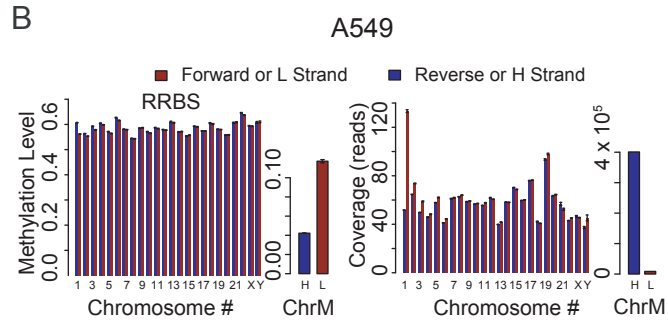
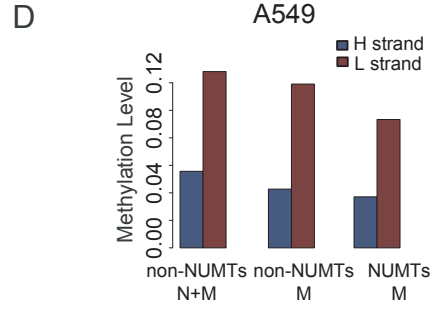
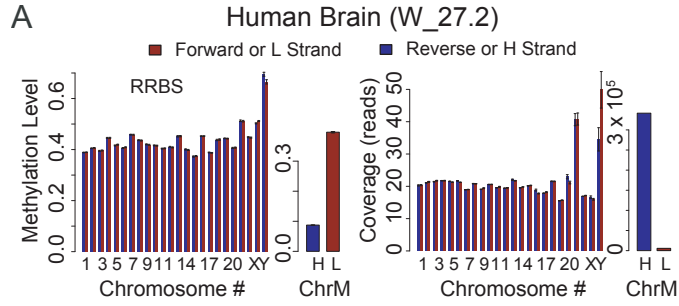
(B) Heat map of correlation (CSI) between mean methylation levels on each pair of functional elements for 14 human PFC samples including regulatory regions (red), tRNA (blue), rRNA (yellow) and protein coding gene (green) within H or L strand. Elements are hierarchically clustered.

(C) Mean methylation levels on each category of functional element for 14 human PFC on the H and L strand. Error bars represent the SEM among functional elements in PFC samples.

(D) Range of DNA methylation levels for 14 human PFC samples across mtDNA per 50 bp on the H strand and L strand. Vertical lines (grey) show the 25<sup>th</sup> percentile and 75<sup>th</sup> percentile of methylation level across PFC samples, and stars represent the mean of the methylation level across 14 human PFC samples.

(E) Mitochondrial transcript abundance levels in reads per kilobase per million mapped reads (rpkm). Error bars represent SEM among 9 PFC samples.





**Supplemental Fig. 4. Evaluating different WGBS methods in detection of mtDNA methylation.**

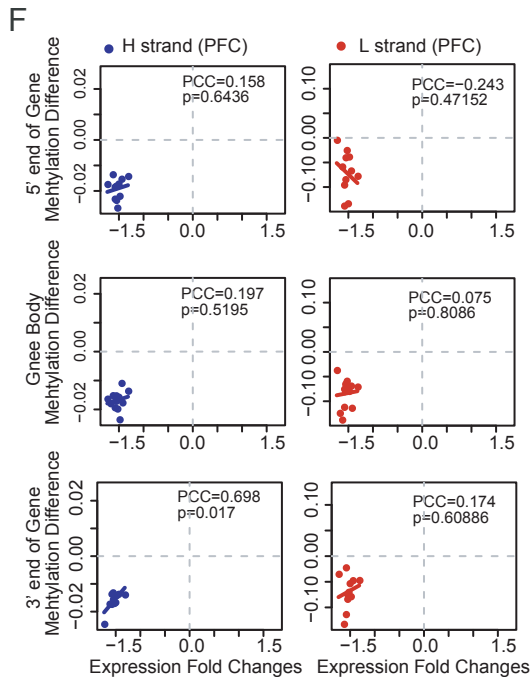
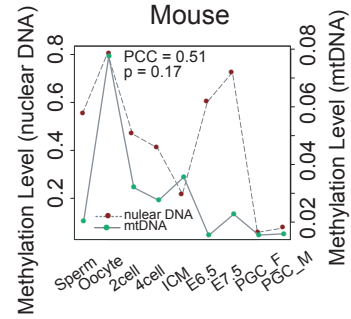
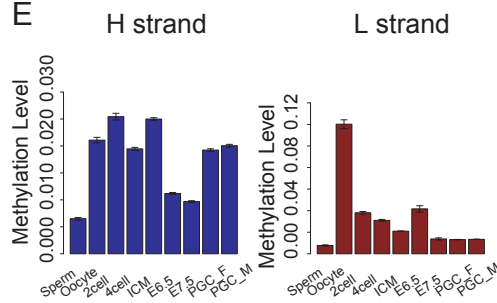
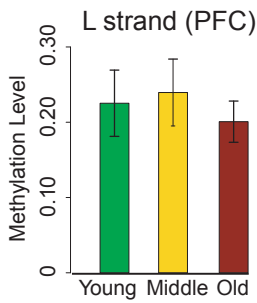
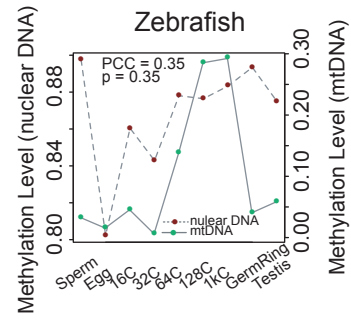
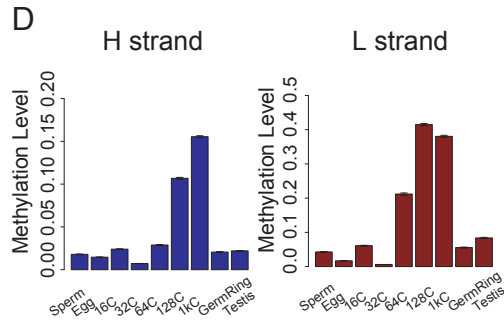
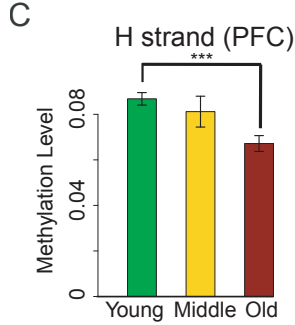
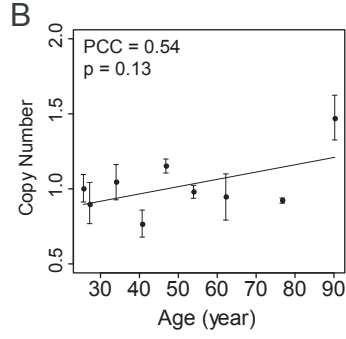
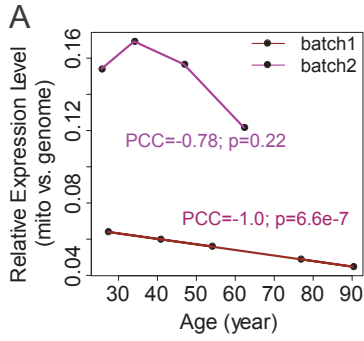
(A) Methylation levels and sequence depth across all chromosomes and mtDNA in a representative PFC sample. Error bars represent the SEM among methylated CpG sites in autosomes or methylated C sites in ChrM.

(B) Methylation levels and sequence depth across all chromosomes and mtDNA in A549 cells. Error bars represent the SEM among methylated CpG sites in autochromosomes or methylated C sites in ChrM.

(C) Methylation levels and sequence depth across all chromosomes and mtDNA for two mouse ESC samples (d0 and d6 obtained from published datasets GSE48229). Error bars represent the SEM among methylated CpG sites for autosomes or methylated C sites for ChrM.

(D) Methylation level of non-NUMTs mapping with N+M (nucleus plus mitochondria) or only M (mitochondria), NUMTs mapping with M in A549 cells on the H and L strand separately. Error bars represent SEM among C sites covered by at least ten reads.

(E) Hierarchical clustering of PFC samples (columns) based on the methylation level of each C site on the H strand (up) and L strand (bottom) before and after ComBat normalization. Rows are Z-score normalized, and columns are clustered based on Euclidean distance.



**Supplemental Fig. 5. mtDNA methylation decreases during aging and is negatively correlated with gene expression.**

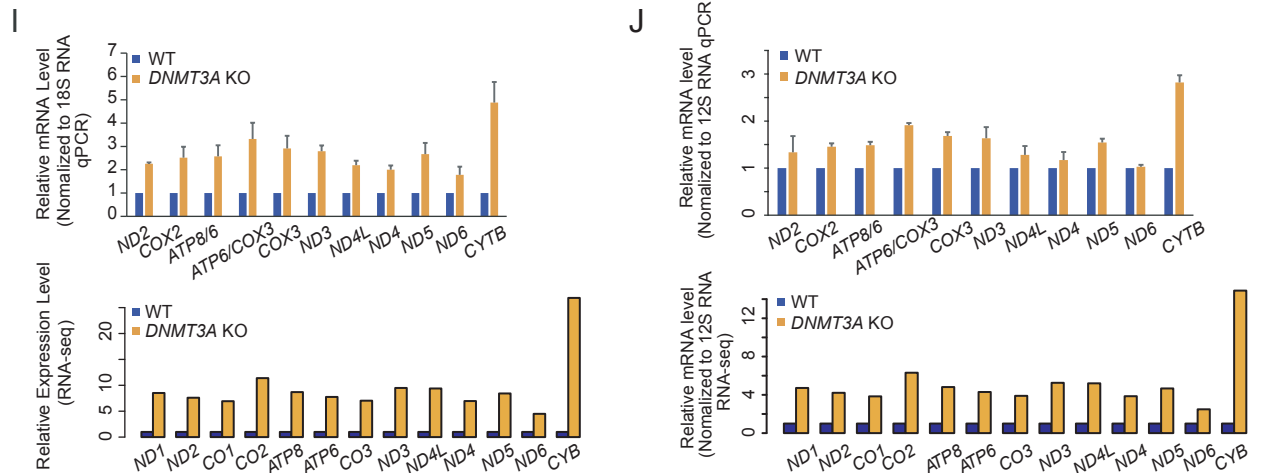
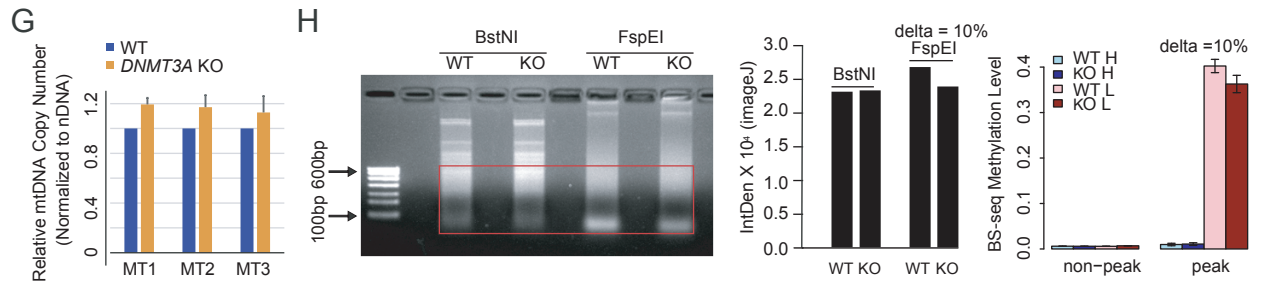
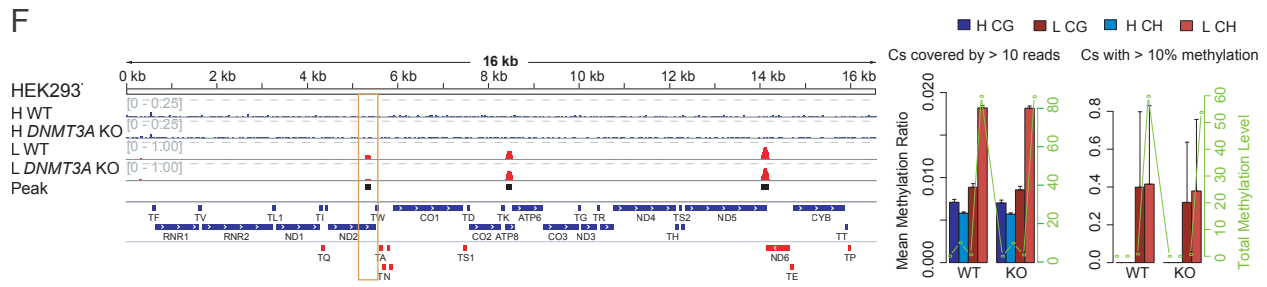
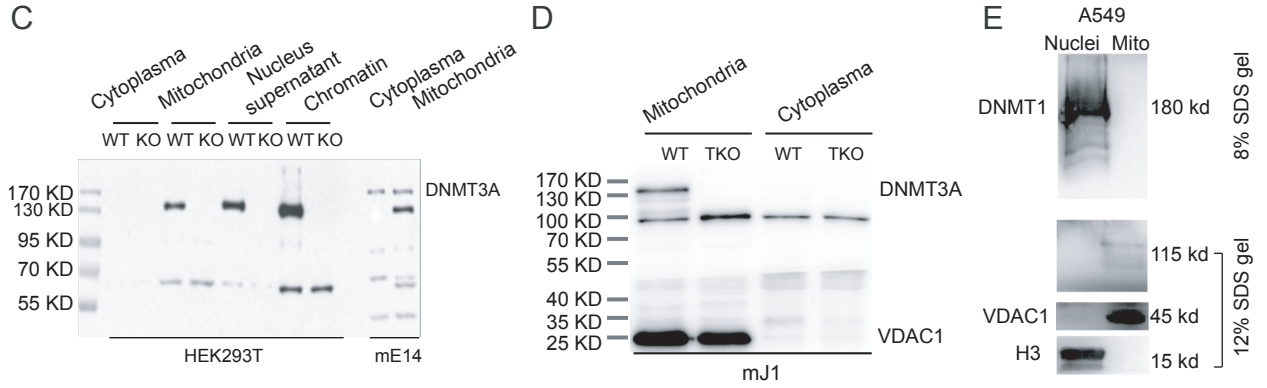
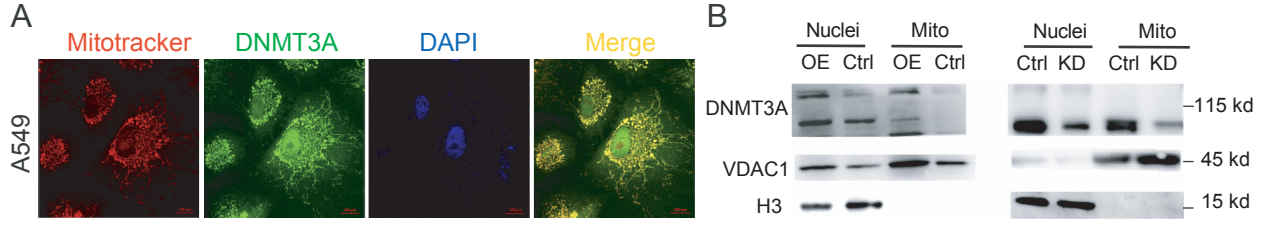
(A) Relative mean mitochondrial transcript abundance with age, based on RNA-seq data for 9 of the 14 PFC samples, and normalized by copy number shown in (B).

(B) mtDNA copy number over age range of samples. Error bars represent the SEM of three technical replicates.

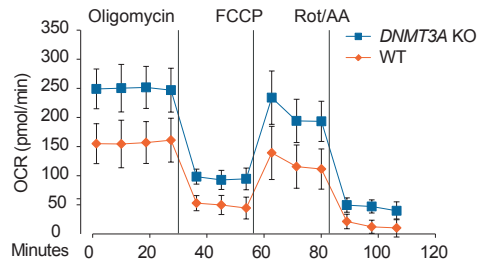
(C) Mean methylation levels for samples grouped into young (20-40 years), middle age (40-60 years), and old (>60 years) on the H and L strand. \*\*\* indicates one sided *t*-test p value < 0.001. Error bars represent SEM within young (5 PFC samples), middle age (4 PFC samples) and old (5 PFC samples).

(D, E) Mean methylation on mtDNA H (left panel) and L (middle panel) strands, and nuclear DNA (right panel), respectively, during zebrafish (D) and mouse (E) early embryogenesis. Error bars represent SEM among all detected C sites.

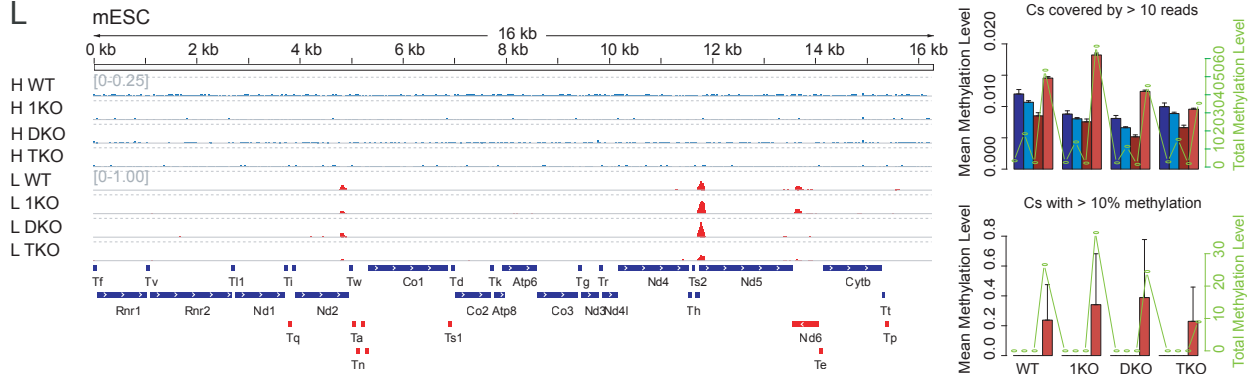
(F) Scatter plot of expression fold changes (FC) against H and L strand methylation difference of 5' end (+/-200bp of TSS), gene body and 3' end (+/- 200bp of TTS) of genes comparing Old with Young.



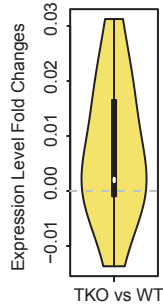
### K HEK293T Oxygen Consumption



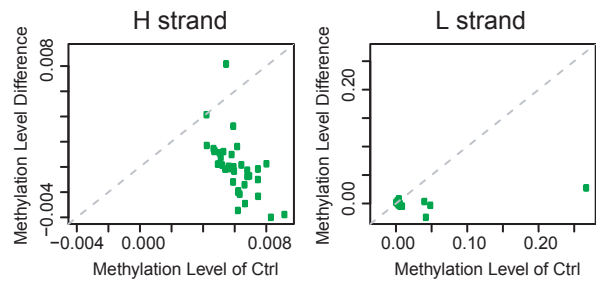
### L



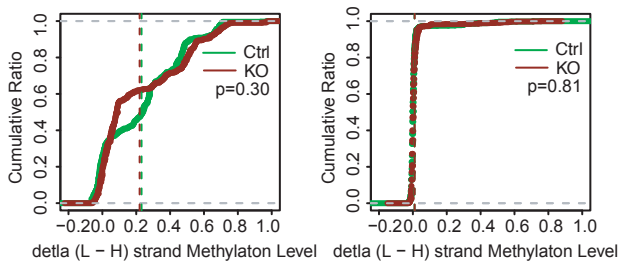
### M



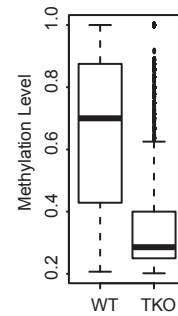
### N



### O



### P



**Supplemental Fig. 6. Effect of *DNMT3A* KO on mtDNA copy number and gene expression.**

(A) Immunofluorescence staining of DNMT3A. Cells were exposed to MitoTracker Orange (red) to label mitochondria and anti-DNMT3A (green) and DAPI (blue) to label nuclei.

(B) Western blots of DNMT3A in *DNMT3A* OE (left panel) and KD (right panel) A549 cells and their corresponding controls. Cells were separated into nuclear and mitochondria fractions, and probed with anti-DNMT3A and VDAC1 as an internal mitochondria protein control and H3 as a nuclear protein control.

(C) Western blots of DNMT3A in both WT and *DNMT3A* knockout HEK293T cells, WT mouse E14. WT and *DNMT3A* KO HEK293T cell were separated into different components including cytoplasm, mitochondria, nucleus supernatant and chromatin, and mouse E14 cells were separated into cytoplasm and mitochondria, and probed with anti-DNMT3A.

(D) Western blots of DNMT3A in WT and TKO mouse J1 cells. J1 cells were separated into mitochondria and cytoplasm fractions, and probed with anti-DNMT3A and VDAC1 as an internal mitochondria protein control.

(E) Western blots of DNMT1 in WT A549. A549 cell were separated into nuclei and mitochondria, and probed with anti-DNMT1, and VDAC1 as an internal mitochondria protein control and H3 as nuclei control.

(F) Left panel, mtDNA methylation profiles of WT and *DNMT3A* KO HEK293T cell on the H and L strand. Blue tracks show H strand methylation levels (scale from 0 to 0.25) and red tracks show L strand methylation (scale from 0 to 1). Middle annotations show mtDNA elements: in blue are polypeptide genes, rRNA and tRNAs coded on H strand; in red are polypeptide genes and tRNAs coded on L strand. Right panel, summary statistics as annotated in Figure. 1.

(G) Relative copy number of mtDNA in WT and *DNMT3A* KO HEK293T cells. Error bars represent standard error among the three replicates.

(H) Gel electrophoresis of mtDNA (ug/reaction) digested by BstNI and FspEI in WT and *DNMT3A* KO HEK293T cells (left panel). Quantification (IntDen) of DNA smaller than 600 bp using ImageJ (middle panel). Mean mtDNA methylation of WT and *DNMT3A* KO HEK293T cells in non-peak and peak (F) regions on H or L strand. Error bars represent SEM among all detected C sites (right panel).

(I) Mitochondria gene expression level relative to 18S RNA by qPCR (top panel) and log<sub>2</sub> transformed RPKM by RNA-seq (bottom panel) in WT and *DNMT3A* KO HEK293T cells. Primers are listed in Table S8.

(J) Mitochondria gene expression level relative to 12S rRNA in WT and *DNMT3A* KO HEK293T cells by qPCR (top panel) and RNA-seq (bottom panel). Primers are listed in Table S8.

(K) Oxygen consumption of *DNMT3A* KO with WT HEK293T cells. Oxygen consumption represents basal respiration, followed by the respiration after ATP synthase inhibition by oligomycin, maximal respiration induced by FCCP, and total block of mitochondrial-respiration by rotenone/antimycin A (Rot/AA).

(L) Left panel, mtDNA methylation profiles of WT, *Dnmt1* KO (single KO, KO), *Dnmt3a/Dnmt3b* KO (double KO, DKO), and *Dnmt1/Dnmt3a/Dnmt3b* knockout (triple KO, TKO) mouse ESC on the H or L strand. Blue tracks show H strand methylation levels (scale from 0 to 0.25) and red tracks show L strand methylation (scale from 0 to 1). Middle annotations show mtDNA elements: in blue are polypeptide genes, rRNAs and tRNAs coded on H strand; in red are polypeptide genes and tRNAs coded on L strand. Right panel, summary statistics as annotated in Figure. 1.

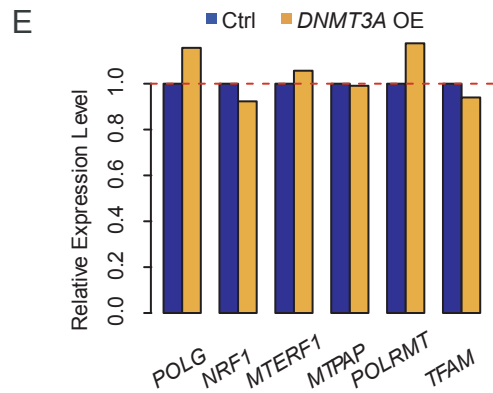
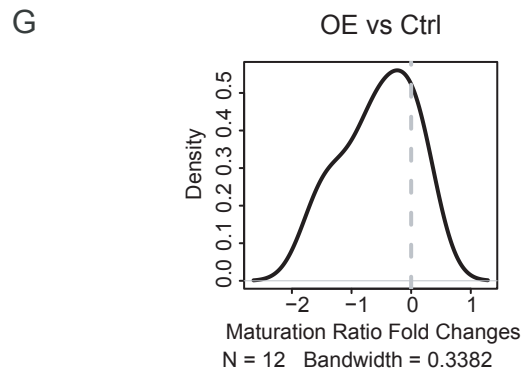
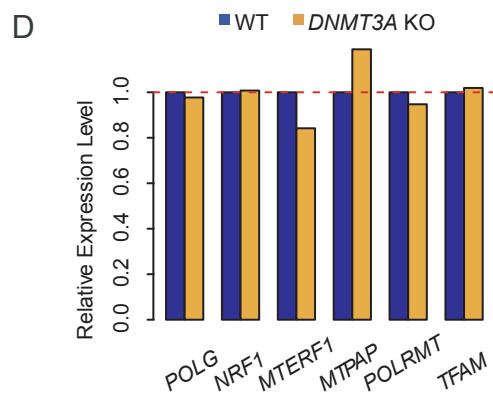
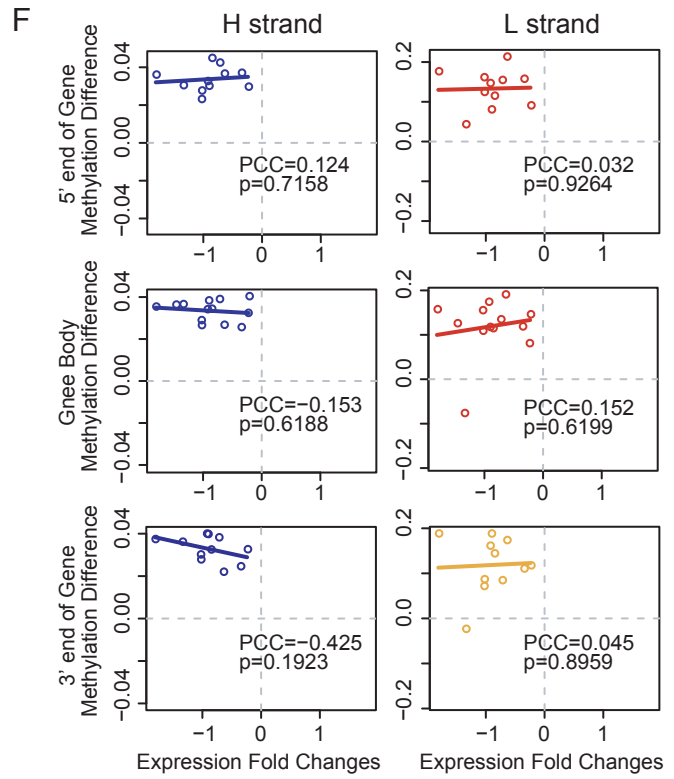
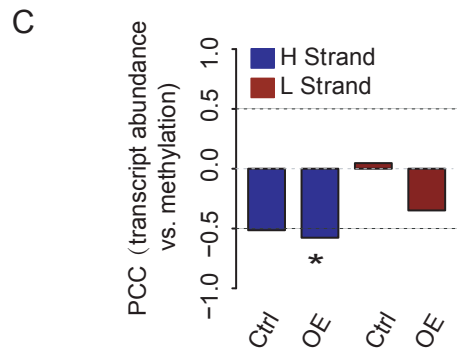
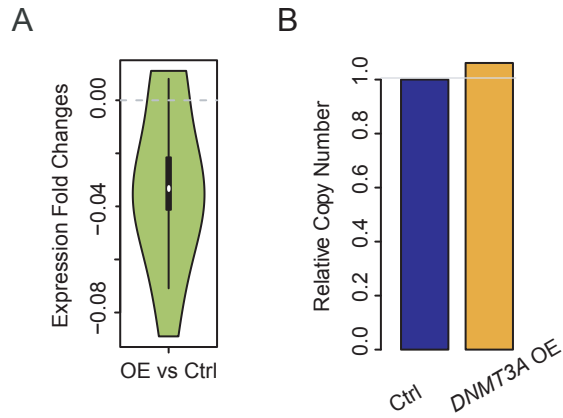
(M) Violin plot of mitochondrial gene expression level relative to 12S rRNA changes comparing TKO with WT J1 mESCs.

(N) Scatter plot between mean methylation level of 63 functional elements of control samples (x-axis) and corresponding methylation level difference between *DNMT3A* KO and control samples (y-axis) on H and L strand.

(O) Cumulative curve of methylation level difference between L and H strand of C sites that contain methylation sum of Ctrl and KO  $> 0.05$  (left panel) or  $> 0$  (right panel) after sampling 1000 paired Cs under *DNMT3A* KO. The p value for the difference between *DNMT3A* KO and control was calculated with a one-sided *t*-test.

(P) Methylation levels of CpG sites with methylation ratio  $> 0.2$  and coverage  $> 5$  in both WT and TKO J1 mESC on nuclear DNA.





**Supplemental Fig. 7. Effect of *DNMT3A* OE on mtDNA copy number and gene expression.**

(A) Violin plot of expression fold changes comparing *DNMT3A* OE with control A549 cells.

(B) Relative mtDNA copy number in *DNMT3A* OE with control A549 cells. mtDNA copy number was estimated by reads mapped to mtDNA relative to nuclear DNA after normalizing their nucleotides coverage, respectively.

(C) Correlation between transcript abundance and mean gene body methylation level across genes within each sample on the H and L strand.

(D-E) Expression level of key nuclear encoded mitochondrial regulatory factors comparing *DNMT3A* KO (D) and *DNMT3A* OE (E) with their corresponding controls in HEK293T and A549 cells respectively.

(F) Scatter plot of expression fold changes (FC) against H and L strand methylation difference of 5' end (+/-200bp of TSS), gene body and 3' end (+/- 200bp of TTS) of gene comparing *DNMT3A* OE with control. \* denotes negative PCC with  $p < 0.01$ .

(G) Density plot of maturation ratio fold changes comparing between *DNMT3A* OE with control.